J. Mech. Phys. Solids Vol. 32, No. 4, pp. 443–460, 1984.
Printed in Great Britain.

0022–5096/84 $3.00 + 0.00

THE DETERMINATION OF DYNAMIC FRACTURE TOUGHNESS OF AISI 4340 STEEL BY THE SHADOW SPOT METHOD

A. J. ROSAKIS,† J. DUFFY and L. B. FREUND
Division of Engineering, Brown University, Providence, RI 02912 U.S.A.

(*Received* 20 *February* 1984)

ABSTRACT

DYNAMIC crack propagation experiments have been performed using wedge loaded double cantilever beam specimens of an austenitized, quenched and tempered 4340 steel. Measurements of the dynamic stress intensity factor have been made by means of the optical method of caustics. The interpretation of experimental data, obtained from the shadow spot patterns photographed with a Cranz–Schardin high speed camera, is based on an elastodynamic analysis. The instantaneous value of the dynamic stress intensity factor K_I^d is obtained as a function of crack tip velocity. Finally, the interaction of reflected shear and Rayleigh waves with the moving crack tip stress field is considered.

1. INTRODUCTION

A VARIETY of criteria based on the results of stress analysis of cracked solids and on the experimental evaluation of the fracture behavior of real materials can be imposed in the safe design of structures. For proper material selection, the general performance characteristics of the material class under consideration must be known. If the fracture initiation resistance of materials were always to increase with loading rate and if crack propagation resistance were independent of crack tip speed, then quasi-static tests could be used to establish material parameters for design. This is not the case, however, for some structural materials and it is thus necessary to perform dynamic initiation and propagation experiments for proper characterization of the materials. Even in cases where the loading is quasi-static, behavior similar to that which occurs under rapid loading may be exhibited at the tip of a dynamically propagating crack due to the higher strain rates present locally. Thus, for structural materials, both the fracture initiation and subsequent propagation must be taken into account; and with a view toward crack arrest criteria, the resistance of the material to rapid crack propagation must be known also. A dynamic fracture criterion based on the stress intensity factor may be expressed as a simple generalization of the familiar static criterion. This is done by the introduction of a time dependent amplitude factor $K_I^d(t)$ as a feature of a transient

† Now at the Division of Engineering and Applied Science, California Institute of Technology, Pasadena, CA 91125.

stress field and an experimentally determined critical value K_{Ic}^{d} that is assumed to be a material property.

For a propagating crack the fracture criterion is assumed to take the form

$$K_I^d = K_{Ic}^d(v)$$

where v is the instantaneous crack-tip speed. The actual dependence of K_{Ic}^{d} on v must be determined by experiment.

Direct optical methods based on light wave interference have been used in the past few decades for the study of stress fields in the vicinity of dynamically propagating cracks in nominally elastic materials. Through their application, important advances in the study of rapid fracture have been made, in particular by DALLY (1979) and by KOBAYASHI (1970, 1978). However, these methods are restricted to transparent materials unless one adopts the method put forward by KOBAYASHI and DALLY (1980) in which opaque materials are covered with transparent coatings. MANOGG (1964) introduced the method of caustics, a technique based on geometrical optics, and also known as the shadow spot method. Through such contributions as those of THEOCARIS and GDOUTOS (1972), BEINERT and KALTHOFF (1979), RAVI-CHANDAR (1982) and RAVI-CHANDAR and KNAUSS (1982) this method has become established as a standard procedure for the measurement of dynamic fracture toughness of nominally elastic transparent materials. It has the advantage over other methods of providing a direct measure of the crack tip field and the corresponding crack tip speed independently of the geometry of the specimen, the detailed boundary conditions, or the complex stress wave pattern in the specimen. In addition, within the past few years, ROSAKIS (1980) and ROSAKIS and FREUND (1981, 1982) provided analyses to account for the effects of material inertia and crack tip plasticity in the interpretation of shadow spot data obtained with light reflected from specimens of opaque structural materials.

The present paper presents a description of dynamic crack propagation experiments on double cantilever beam specimens of a high strength steel. Measurements of the crack tip deformation field and of crack speed during propagation have been made using the optical method of caustics in reflection. Initially, this method was used in experiments involving rapid crack propagation and stress wave loading by BEINERT and KALTHOFF (1979) and more recently by GOLDSMITH and KATSAMANIS (1979). In each case it was assumed that the elastic stress field near the tip of a rapidly propagating crack in a nominally elastic solid has precisely the same spatial variation as the elastic plane stress field near the tip of a stationary crack. More recently, both KALTHOFF *et al.* (1979) and ROSAKIS (1980) reanalyzed the method as applied in dynamic fracture to estimate the effect of material inertia on inferred values of stress intensity factor. Furthermore, a first attempt to incorporate both inertia effects and crack tip plasticity effects in the analysis underlying the use of the method was presented by ROSAKIS and FREUND (1981). This work resulted in estimates for the limits of applicability of the quasistatic elastic model as a basis of the method.

In the work described here, the shadow spot patterns corresponding to dynamically propagating and subsequently arresting cracks have been photographed with a high speed camera of the Cranz–Schardin type. The instantaneous value of the dynamic stress intensity factor K_I^d and of crack length are obtained at several different times, and the variation of fracture toughness with crack speed is inferred.

For a propagating crack, the instantaneous value which the stress intensity factor assumes is the dynamic fracture toughness. The results of the present experiments show that dynamic fracture toughness is an increasing function of crack tip speed for the 4340 steel tested. This behavior is consistent with the predictions of a theoretical analysis presented by FREUND and DOUGLAS (1982) and DOUGLAS (1982) of dynamic elastic–plastic crack growth in a strain rate independent material under conditions of contained yielding according to a critical plastic strain crack growth criterion.

The experimental results show that the stress intensity factor and the corresponding crack tip speed undergo abrupt changes during the growth process. It is possible that these changes are due to stress waves which are emitted from the crack tip when it suddenly begins to grow, and which are subsequently reflected back onto the moving tip from the boundaries of the specimen. These variations, which complicate the analysis of the experimental data, have been interpreted in terms of simple analytical models of cracks propagating rapidly in DCB (double cantilever beam) specimens. Because of the uncertainties involved, however, this analysis is somewhat speculative at the present time.

2. THE FORMATION OF SHADOW SPOTS BY REFLECTION

For opaque specimens the optical shadow spot pattern is formed by the reflection of light from the polished specimen surface. We consider a planar specimen occupying a region of the x_1, x_2 plane and of uniform thickness d in the undeformed state. The specimen contains an edge crack and is subjected to specified in-plane tractions and/or displacements along its outer boundary. Under load, the change in thickness in the vicinity of the crack tip is non-uniform and the equation of the deformed specimen surface is given by

$$x_3 = -f(x_1, x_2). \tag{1}$$

As shown in Fig. 1, if a beam of parallel light rays travelling in the x_3 direction is normally incident upon the deformed specimen surface, then, upon reflection, the light rays no longer will be parallel. Furthermore, if certain geometric conditions are met by the reflecting surface as described below, then the virtual extensions of the reflected rays will form an envelope describing a three-dimensional surface in space. This surface, called the *caustic surface*, is the locus of points of maximum luminosity. Its intersection with a plane parallel to the specimen defines the caustic curve, which can be recorded photographically. For this purpose a camera is positioned in front of the specimen and focused onto the "screen", at a distance z_0 behind the plane of the undeformed specimen; see Fig. 1. The reflected light field provides an image of the caustic curve surrounding the shadow spot at the focal plane of the camera.

A convenient method of finding the equation of the caustic curve involves the mapping of points x_i of the reflecting surface on to points X_i of the "screen". These two sets of coordinate axes are parallel, respectively, to one another and separated by a distance z_0. When the incident light rays are reflected from the point x_i their virtual extensions will intersect the "screen" at the image point X_i, as shown in Fig. 1. The

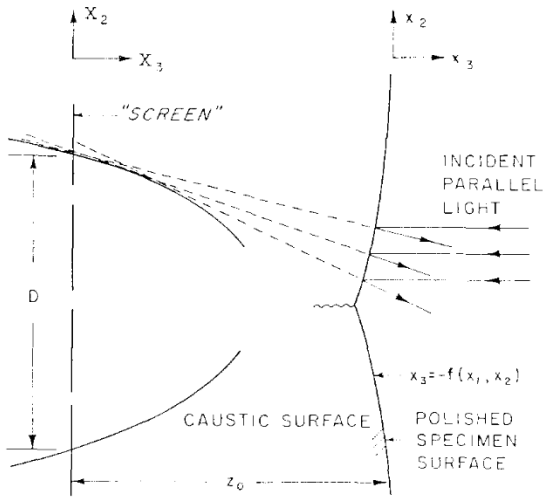

FIG. 1.

equations of the mapping were first derived by MANOGG (1964), who showed that

$$X_i = x_i \pm 2z_0 \, \partial f/\partial x_i, \tag{2}$$

where f, the lateral contraction of the specimen is given by (1), and where the choice of sign depends on whether the image is real or virtual (a positive sign for transmission caustics and a negative sign for reflection caustics). It should be noted that the mapping equations for arbitrarily large deformation of the reflecting surface reduce to (2) when both $|f/z_0|$ and $|\partial f/\partial x_i|$ are small compared to unity; this result was contained in the work of ROSAKIS (1982).

As can be seen in Fig. 1, the caustic curve is the intersection of the caustic surface with the plane on which the camera is focused, i.e. with the "screen". The mapping represented by (2) is not invertible for those points lying on the caustic curve, and the Jacobian determinant of the transformation must vanish at those points which map into the caustic curve according to (2), that is,

$$J(x_1, x_2) \equiv \frac{\partial(X_1, X_2)}{\partial(x_1, x_2)} = 0. \tag{3}$$

The *initial curve* may be defined as the locus of points on the specimen for which $J(x_1, x_2) = 0$. Thus the caustic, which is the curve of high luminosity on the "screen", corresponds to reflections from the vicinity of the initial curve on the specimen. This property gives the initial curve considerable significance. The size of the initial curve relative to that of the plastic zone plays an important role in the analysis of caustics in the presence of crack-tip plasticity. Since the initial curve represents those points responsible for the generation of the caustic, its position in relation to the plastic zone will determine the type of information obtained on the "screen".

The dynamic crack propagation experiments described below were performed under conditions of small scale yielding with a plastic zone diameter of approximately 2 mm.

Special care was taken to ensure that the size of the initial curve was at least twice that of the plastic zone. As shown by ROSAKIS and FREUND (1981), this size requirement must be met in order that an elastic dynamic analysis of the caustic pattern be valid. For elastic deformation of a plate of uniform thickness d in a state of plane stress, the deformed shape of the reflecting surface in (2) is given by:

$$f(x_1, x_2) = \nu d(\sigma_{11} + \sigma_{22})/2E, \tag{4}$$

where ν is Poisson's ration, E is the elastic modulus, and $\sigma_{11} + \sigma_{22}$ is the first stress invariant. By making use of the results cited above, one can show that for steady dynamic growth of a tensile crack under plane stress conditions,

$$\sigma_{11} + \sigma_{22} = -(1+\nu)v^2\rho \frac{K_I^d(1+\alpha_s^2)}{\mu Q} Re[2\pi z_l]^{1/2}, \tag{5}$$

where ρ is the material mass density, v is the speed of crack growth, μ is the elastic shear modulus, $z_l = x_1 + ix_2\alpha_l$, and $Q = 4\alpha_s\alpha_l - (1+\alpha_s^2)^2$. The parameters α_l and α_s can be evaluated through the equations $\alpha_{l,s} = (1 - v^2/c_{l,s}^2)^{1/2}$, where c_l and c_s are the longitudinal and shear elastic wave speeds, respectively.

The equation of the caustic curve is then obtained by substituting equations (4) and (5) into the optical mapping (2) and by imposing the condition for the existence of a caustic curve, given by (3). Finally, the instantaneous value of the dynamic stress intensity factor can be expressed as a function of the maximum transverse diameter D of the caustic curve as

$$K_I^d(t) = C(\alpha_l) \frac{2(2\pi)^{1/2} E[4\alpha_l\alpha_s - (1+\alpha_s^2)^2]}{z_0 \nu d(1+\alpha_s^2)(\alpha_l^2 - \alpha_s^2)} D^{5/2}. \tag{6}$$

As shown by MA (1982), the coefficient $C(\alpha_l)$ in this expression can be approximated quite accurately by $C(\alpha_l) = (6.8 + 14.4\alpha_l - 2.6\alpha_l^2) \times 10^{-3}$. Expression (6) was used throughout the present paper in the interpretation of the results of the dynamic propagation experiments performed with the 4340 steel specimens.

3. THE DYNAMIC CRACK PROPAGATION EXPERIMENTS

The specimens used in this investigation were of the single edge crack configuration commonly known as the double cantilever beam, or DCB. Since this geometry is one frequently employed both in analytic and in experimental fracture investigations, its adoption here makes it possible to compare present results with those of other investigators as for instance KANNINEN (1978) or NISHIOKA and ATLURI (1982). The specimens were machined from steel plate of commercial AISI 4340 steel. Their final dimensions were 229 mm by 76 mm, with a thickness of 12.7 mm. The precrack, which is introduced by means of a spark cutter, runs along the center line of each specimen to a length of 63.5 mm and ends at a 1.40 mm drilled hole. Figure 2 shows the experimental arrangement, including the two wedges used to force open the crack. These wedges bear on two hardened steel pins of 16 mm diameter, one in each arm of the specimen. During a test, the wedges are brought down by a slow-moving hydraulic ram, while the other end of the specimen is clamped on a firm base.

There are a number of advantages in the experimental method adopted. Since the crack tip is blunted by the drilled hole, a load greater than that needed to grow a sharp crack is required before the onset of fracture initiation, resulting in a relatively high initial crack speed. Thus the range of this study includes higher crack speeds. In addition, in this experimental configuration the crack grows into a region of decreasing load intensity so that, under suitable conditions, the fracture can be arrested within the specimen before it is completely divided. Finally, as shown by COTTERELL and RICE (1980), this mode of loading results in a crack which usually grows along a fairly straight line down the center of the specimen, thus avoiding a curved crack which would make interpretation of the caustic patterns difficult.

The material heat treatment consisted of austenitizing at 843°C (1550°F) for 1 h, followed by an oil quench and a temper to 316°C (600°F) for 1 h. After this heat-treatment, the crack was spark-cut to the drilled hole, then one face of the specimen was ground, lapped and polished to produce a surface with high reflectivity and a high degree of flatness. In separate tests, it was determined that the flow stress of this material in tension is approximately 1300 MPa and that it has a hardness of 45 on the Rockwell C scale.

The caustic patterns formed during the course of the experiments were recorded by means of a high speed camera of the Cranz–Schardin type. The present camera employs twelve flash tubes arranged in a 3×4 array, as shown schematically in Fig. 3, to provide the light sources for a sequence of twelve pictures. Each flash has an effective duration of approximately 1 μs. To obtain a predetermined time interval between flashes, each flash tube is triggered separately, within the range 0.8 to 740 μs. As indicated in the figure the light from the flash tubes strikes a parabolic mirror which then directs it onto the polished surface of the specimen. Upon reflection from this surface, the light rays converge and are focused on the twelve objective lenses of the camera. Each of these lenses, whose focal length is 660 mm, corresponds to one of the flash tubes. The

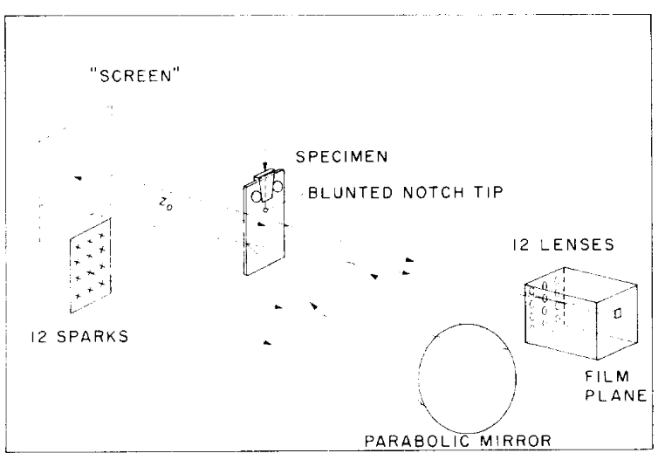

FIG. 3.

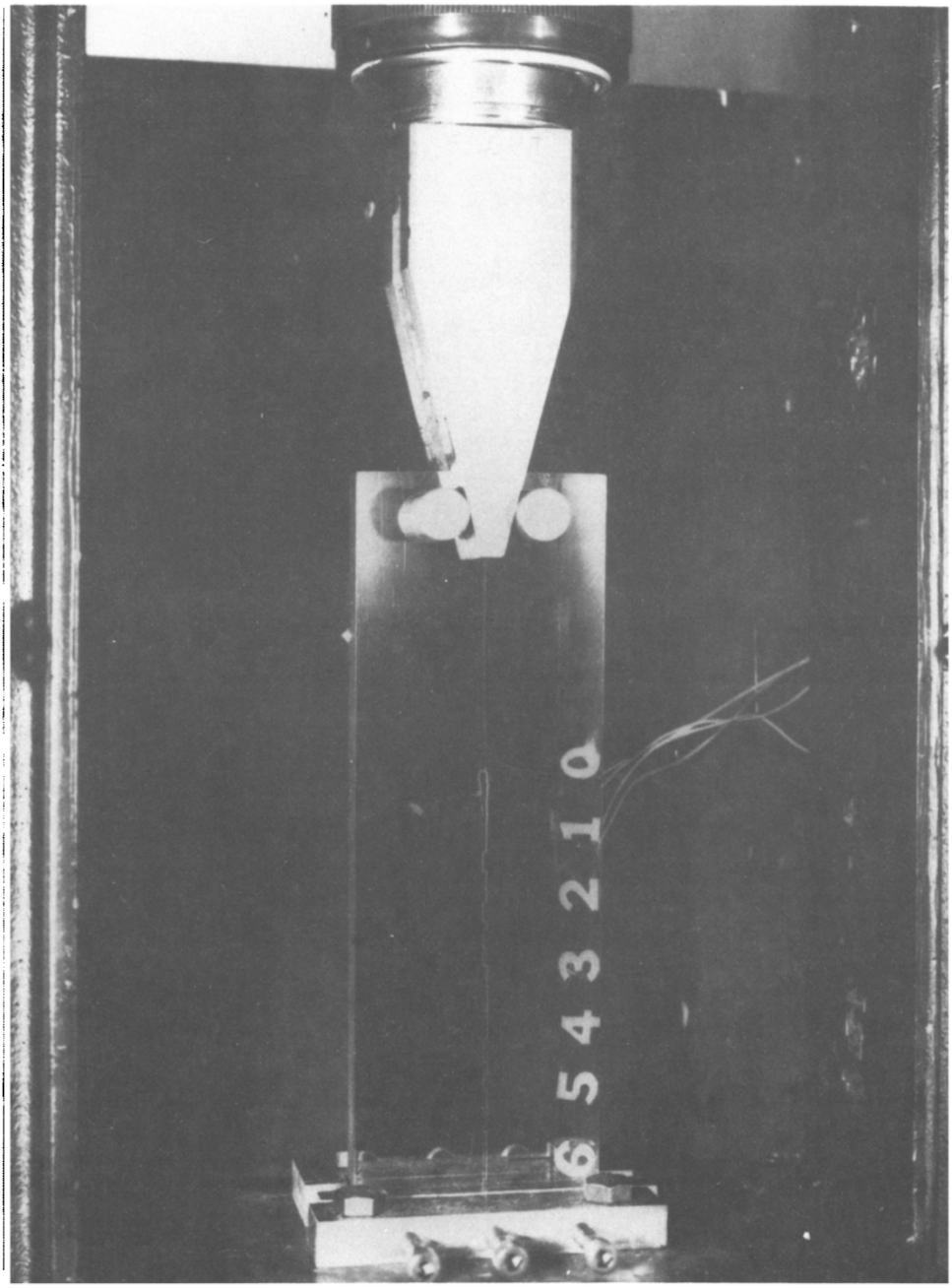

FIG. 2.

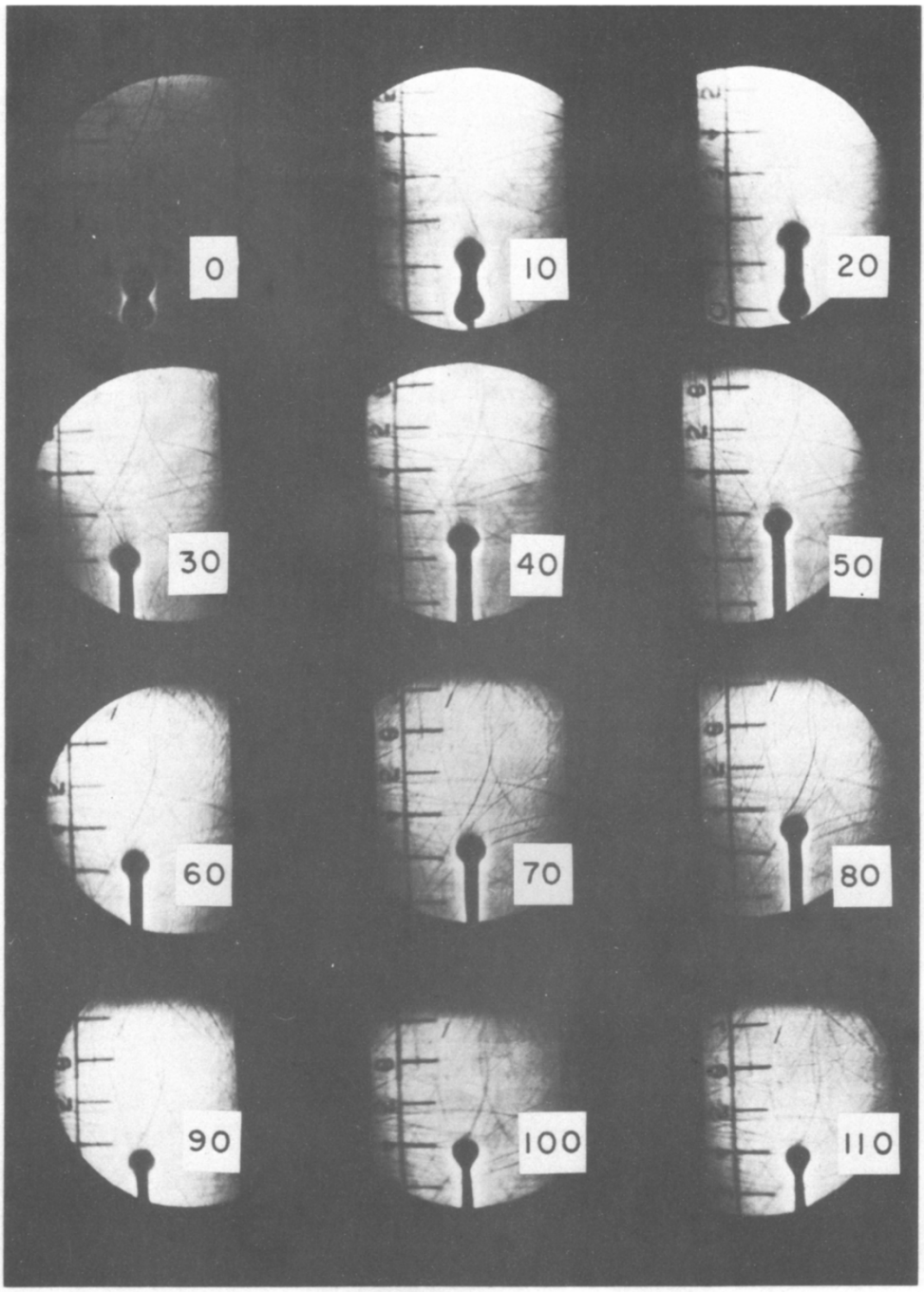

DYNAMIC CAUSTIC PATTERNS OBTAINED BY REFLECTION (4340 STEEL, 1550°F, O.Q. 600°F)

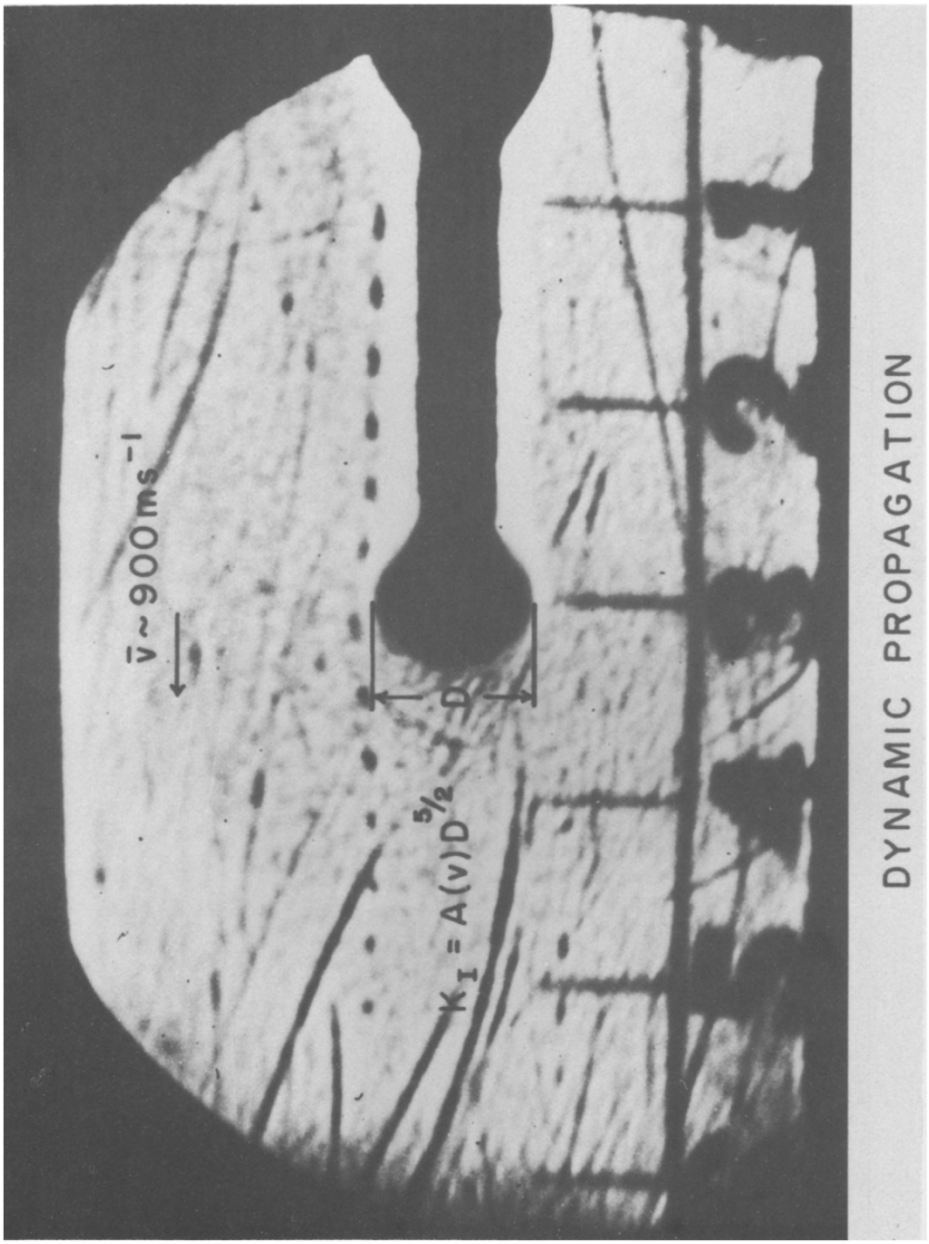

FIG. 5.

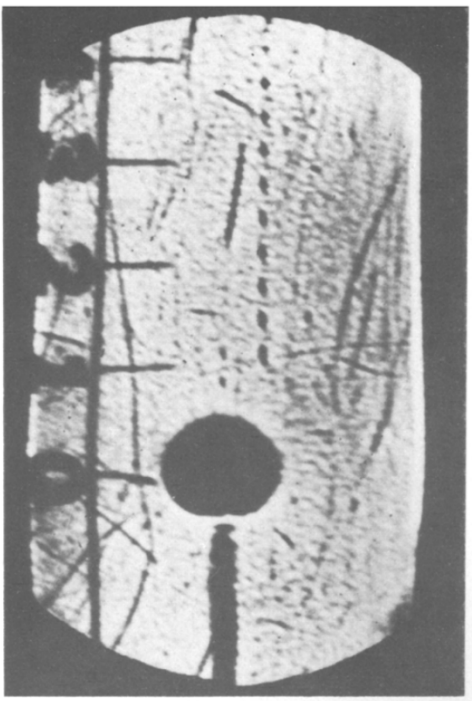

Static loading

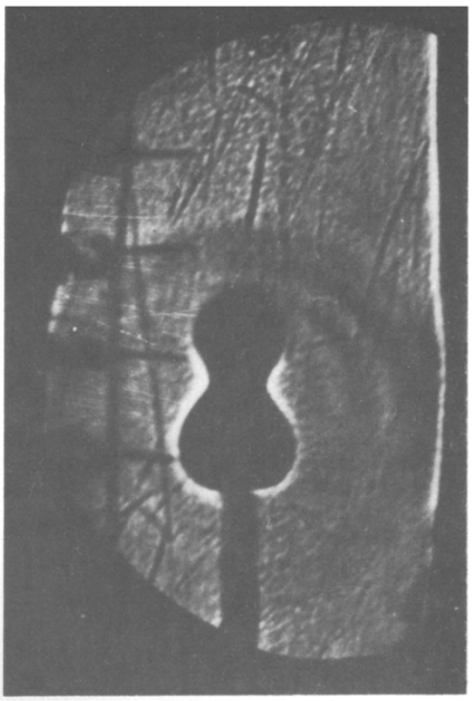

Dynamic initiation

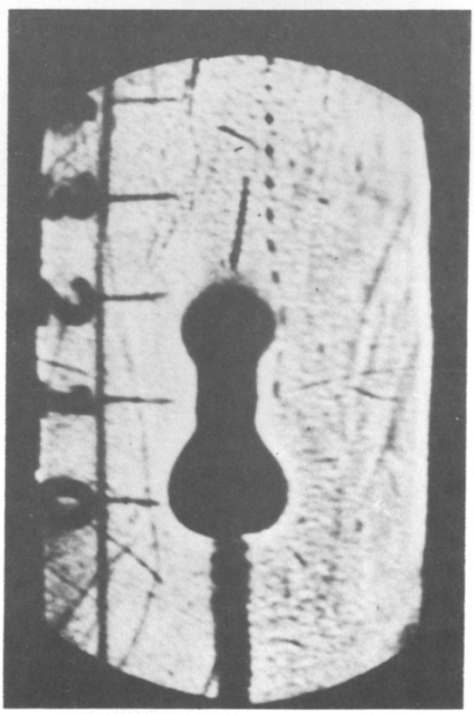

Dynamic propagation

camera is focused to a plane behind the specimen, indicated by "screen" on the diagram.

During a test, when the load supplied by the wedge reaches a critical value, a sharp crack starts to propagate from the notch tip. The camera is then triggered by the crack itself as it starts to move and breaks a conducting strip cemented to the reverse side of the specimen. This conducting strip is placed at the crack tip perpendicular to the anticipated fracture path. As the crack advances the reflective surface of the specimen deforms and a series of twelve caustic patterns is recorded sequentially on $8'' \times 10''$ photographic film, Fig. 4. In the resulting photograph, each image of the specimen measures 25 by 35 mm, and shows a shadow spot and a caustic curve surrounding the moving crack tip. An enlargement of one of these images is shown in Fig. 5.

After completing a test, two measurements are made from each image to provide values of the stress intensity factor and the corresponding crack speed. The average speed between frames is calculated from the instantaneous position of the crack tip by locating the position of the maximum transverse diameter of each caustic relative to a scale drawn on the specimen surface. In the photographs, this scale appears somewhat blurred. This is because the camera is not focused on the specimen but on a plane behind the specimen, as explained above. The number zero on the scale corresponds to the tip of the blunted notch and the distance between the lines is 20 mm. Since the instant at which each photograph is recorded is known quite precisely, it becomes possible to evaluate the average crack speed between photographs by dividing the change in position of the crack tip by the elapsed time. The second measurement made is that of the transverse diameter D of the shadow spot. This measurement leads to an instantaneous value of the dynamic stress intensity factor in accordance with the dynamic analytical models presented in Section 2, and in particular on the basis of (6).

4. Qualitative Discussion of Results

The photographic records obtained during the course of the dynamic event, coupled with later examination of the fracture specimen, reveal information about the extent of the plastic deformation produced by the propagating crack. This information is crucial to a proper interpretation of the experimental data. In particular, as noted above, the interpretation of a given caustic pattern in terms of fracture parameters depends upon the relative size of the plastic zone to that of the initial curve. If the initial curve lies well outside the plastic zone, then the elastic solution provided by (6) is applicable. On the other hand, if the initial curve lies within the plastic zone, then a plastic analysis of the deformation pattern is needed before the caustic can be used to provide a measure of the stress intensity factor. Such an analysis is not yet available.

As mentioned previously, the size of the initial curve depends on the distance z_0 separating the "screen" and the surface of the specimen. For the crack propagation experiments described, a rather large value of z_0 was employed. A simple calculation, based on present data and similar to that performed by Rosakis and Freund (1982), shows that the initial curve size r_0 varies from a minimum of 3 mm to a maximum of 4.5 mm. Examination of the metal specimen after fracture shows that the width of the wake of residual plastic strains varies from 1 mm to 2 mm in the region corresponding to

crack propagation. If the width of the wake provides a measure of r_p, the radius of the plastic zone, then the ratio r_p/r_0 is less than one half in the region of crack propagation. This implies that the elastic dynamic analysis described in Section 2 is applicable and that K_I^d is given by (6). The situation is different in the vicinity of the blunted crack tip, where the radius of the plastic zone may be as large as 6 mm. In this case the initial curve lies within the plastic zone and the elastic analysis is no longer valid.

The foregoing is demonstrated qualitatively in Fig. 6, where the event of crack initiation is recorded in the first of the pictures. Although not drawn in the photograph, the initial curve lies within the plastic zone. The shape of the observed caustic corresponds quite closely to that predicted by MA (1982) on the basis of an HRR singular strain field. In the second picture, which was obtained just after initiation, two more or less circular shadow spots appear. The lower spot corresponds to the residual strains left at the site of the notch tip, while the upper spot corresponds to the current location of the crack. In the second, and even more strongly in the third, photograph the two shadow spots are connected by a neck. This neck is the caustic formed by the residual strains left behind in the wake of the propagating crack.

5. QUANTITATIVE DISCUSSION OF RESULTS

In order to analyze the results, the instantaneous crack length $a(t)$ and the dynamic fracture toughness value $K_{Ic}^d(t)$ are plotted as functions of time for each experiment. For all specimens tested, the curves of $K_{Ic}^d(t)$ as a function of time are very similar in nature but are not identical. The main differences are seemingly due to the stress waves which are reflected from the specimen boundaries and interact with the crack tip motion. This interaction produces sudden variations in the crack tip velocity and in the stress intensity factor. The phenomenon will be discussed further in a later section, but it is worth observing here that the curves of $a(t)$ and $K_{Ic}^d(t)$ show oscillations, and that the peaks and jumps in these curves occur at different instants for different tests, depending on the velocity history of the crack tip. It is noted that corresponding results reported for polymers by BEINERT and KALTHOFF (1979) and by KALTHOFF *et al.* (1979) do not show oscillations in the value of K_{Ic}^d and of the crack velocity seen here for metals. This difference may be due to the viscous damping of the waves in the polymer and to the relatively low ratio of specimen stiffness to loading mechanism stiffness in experiments with polymer specimens.

An alternative way of presenting the data is shown in Fig. 7. Here the dynamic fracture toughness and the crack tip velocity are plotted as functions of crack length. Again we observe oscillations in the values of K_{Ic}^d and v to either side of the mean levels indicated by the dotted lines in both curves. The oscillations in K_{Ic}^d and v occur in phase with each other, suggesting the existence of a relationship between K_{Ic}^d and v. Figure 8 shows a plot of K_{Ic}^d as a function of v, obtained from the results of experiments number 8, 9 and 10. The initial crack tip velocity differed in each of these three tests, although the geometry and material properties of the specimens were the same. Figure 8 shows that for values of crack tip velocity less than about 700 ms $^{-1}$, the dynamic fracture toughness is nearly independent of crack velocity. The quasi-static steady growth value predicted here is approximately 50 MN m$^{-3/2}$. But for velocities greater than about 800 ms^{-1} the dynamic fracture toughness increases quite sharply with velocity.

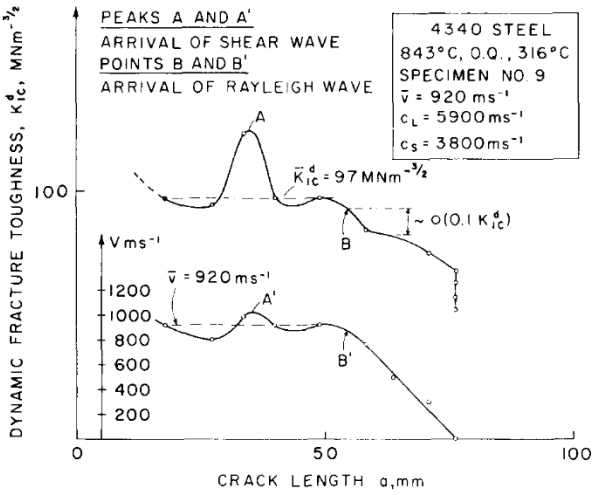

DYNAMIC FRACTURE TOUGHNESS AND CRACK TIP VELOCITY VERSUS CRACK LENGTH.

FIG. 7.

The shadow spot method in reflection mode was used by BEINERT and KALTHOFF (1979) for the study of the arrest process in high-strength steels, but a relation between K^d_{Ic} and v was not reported. For polymers, the available experimental results show a variation of K^d_{Ic} with v that is similar to the one displayed in Fig. 8. However, doubts have been raised by RAVI-CHANDAR (1982) concerning the existence of a single-valued relationship between K^d_{Ic} and v for Homalite 100 and other polymers at very high loading rates.

For crack propagation in a rate-independent material which fractures by the locally ductile mechanism of hole growth under small scale yielding conditions, as is the case

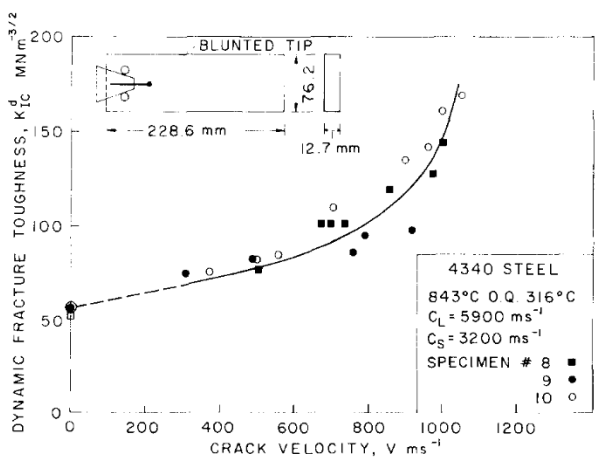

FIG. 8.

here, a quantitative estimate can be made of the influence of material inertia on the relationship between K_{Ic}^d and v. GLENNIE (1972) modified the void growth formulation of RICE and TRACEY (1969) to include the effect of inertia, and he obtained an approximate solution by means of a variational method. The same general line of reasoning is followed here. However, the influence of inertia can be illustrated by means of an elementary argument. Consider the axisymmetric plane strain expansion of a hollow circular cylinder of incompressible material. If the inner and outer radii are instantaneously a and b, respectively, and if the radial speed of the outer surface is u_b, then the radial speed of a material particle at a distance r from the axis of symmetry is u_b/r. Under these conditions, if the material is rigid-plastic with shear flow stress τ_0 and mass density ρ, then the kinetic energy is $T = \rho\pi u_b^2 b^2 \ln(b/a)$ and the rate at which energy is dissipated due to plastic flow is $\dot{W} = 4\pi\tau_0 u_b b \ln(b/a)$ for arbitrary u_b.

To make a connection with the crack growth problem, let δ_s denote the spacing of void nucleation sites on the prospective fracture plane and suppose that initially $b(0) = \delta_s/2$ and $a(0) \simeq 0$. The velocity u_b is prescribed to be that velocity which would cause the hole radius a to grow from essentially zero to $\delta_s/2$ in the time required for the crack tip to advance a distance $\delta_s(1-v^2/c_s^2)^{1/2}$ at speed v. The factor $(1-v^2/c_s^2)^{1/2}$ is included to account for the fact that the region of influence of the crack tip in the direction of growth is contracted because of stress wave effects. Under these conditions, the ratio

$$R = \frac{T+W}{W} = 1 + 0.05\frac{\mu}{\tau_0}\frac{v^2/c_s^2}{(1-v^2/c_s^2)}$$

provides an estimate of the relative influence of inertia in the ductile hole growth process. The simple model could perhaps be pushed one step further to suggest that the relationship between $R^{1/2}$ and v/c_s provides an estimate of K_{Ic}^d divided by the corresponding quasistatic value. For a realistic value of μ/τ_0, say 500, the quantity $R^{1/2}$ has the value 1 if $v/c_s = 0$, 1.9 if $v/c_s = 0.3$, and 3.9 if $v/c_s = 0.6$. Behavior of this type is qualitatively consistent with the data in Fig. 8.

As mentioned in the Introduction, birefringent coatings can be used to provide a direct measure of the instantaneous fracture toughness during crack propagation in opaque materials. This was demonstrated by KOBAYASHI and DALLY (1980) in experiments with compact tension specimens of a 4340 steel. The use of a single coating covering the surface raises questions concerning the relative position of the crack tip in the plastic coating and in the metal specimen. However, KOBAYASHI and DALLY (1980) overcame this problem by using a pair of coatings cemented to the specimen surface one on either side of the crack. As the crack advanced they recorded the isochromatic patterns, from which they calculated the stress intensity at the crack tip as a function of position or of time. For this purpose they employed a high speed framing camera, and they were able to calculate also the crack velocity at each position. Over the range of velocities common to both sets of experiments, the values of K_{Ic}^d for a given velocity are in close agreement. Present values exceed those of Kobayashi and Dally by a consistent 10%. This difference can easily be attributed to different mechanical properties in the two steels due to differences in heat treatment. Of greater significance than the values of K_{Ic}^d is the general shape of the curve. Present results indicate that the stress intensity factor is relatively insensitive to crack tip velocity at lower velocities but becomes greater as the crack tip velocity increases. This is in agreement with the results of

KOBAYASHI and DALLY (1980), and indeed with those based on other methods, as for instance, in the work of DAHLBERG *et al.* (1980).

A second feature of present results that already had been observed by KOBAYASHI and DALLY (1980) are the oscillations in the values of K_{Ic}^d and of v. These oscillations may be due to stress waves reflected from the specimen boundaries which produce change in K_I^d and in v. In the following section, the travel times of stress waves emitted from the accelerating crack tip, and reflected back onto the moving crack from the specimen boundaries, are estimated analytically. The experimental observations suggest a possible correlation between the calculated arrival time of such waves and the observed oscillations in stress intensity factor and crack tip velocity.

6. THE INFLUENCE OF REFLECTED WAVES ON DYNAMIC CRACK ADVANCE

In this section the influence of some of the reflected waves interacting with the propagating crack in a standard DCB specimen is investigated. It is suggested that the abrupt changes that occur both in the velocity and in the stress intensity factor can be explained in terms of such interactions. Simple calculations based on the geometry of the specimen show that the ratio of the specimen compliance to that of the loading system can account for the magnitude of the stress wave-crack interactions.

Exact solutions of the elastodynamic field equations have been found only for the configuration of a semi-infinite crack in an unbounded solid. The results of such analyses are at variance with results of laboratory experiments performed with standard test specimens, as for instance the DCB specimen used in the present investigation. To deal with such cases, stress analyses of dynamic propagation in bounded solids are needed. At the present time, numerical methods are the only means of analyzing most real crack propagation specimen configurations with accuracy. An alternative has been the analysis of simple models which simulate the dynamic process. This approach is especially attractive because most of the important physical features of the problem are retained and the problem is also mathematically tractable. In this section the results of such analyses are compared with experimental data obtained by caustics. The theoretical predictions are found to be qualitatively consistent with the experimental results. Attention is focused mainly on the effects of the shear and Rayleigh waves reflected from the cantilever beam section of the specimen.

In analyzing the DCB specimen, FREUND (1977, 1979) considered a simple model in which the arms of the specimen are constrained to deform as shear beams. In examining the influence of the wave reflection process he concluded that the shear waves reflected from the loading pins back onto the crack tip could significantly influence crack tip motion.

In the formulation of this model two types of boundary conditions were considered. Initially, a perfectly rigid loading system (fixed-grip boundary conditions) was analyzed. The material was assumed to obey a fracture criterion of the form $\Gamma = \Gamma_0$ = constant where Γ is the specific fracture energy. The results show that the crack propagates with a constant speed up to arrest, which coincides with the arrival of the reflected shear wave. In an attempt to make the model more realistic, the assumption of

a perfectly rigid loading apparatus was relaxed. Repeating the analysis for the new condition, the crack was found to propagate with a constant speed until the arrival of the shear wave. At that instant, the crack speed was shown to increase suddenly before decaying eventually to zero. The crack tip acceleration provides an additional amount of crack growth due to the flexibility of the loading apparatus. The ratio of additional crack growth Δl to initial notch length l_0 was found to be a function of the ratio of the flexibility of the specimen to that of the loading device.

Another assumption in the analysis that plays an important role in determining the motion of the crack tip was the specific fracture energy dependence of crack tip velocity. If Γ is a monotonically increasing function of v, and if the loading device is stiff, the crack tip speed will vary in steps, decreasing gradually between fracture initiation and crack arrest. Further consideration of the effect of the flexibility of the loading device produces the result that a series of "steady states" is achieved connected by jumps Δl in crack length attributed to the flexibility of the loading device. The steady-state velocities decrease gradually to zero between initiation and arrest.

The last of the cases discussed above is the most realistic, since both the effects of loading flexibility and material inertia are incorporated. A simple calculation based on the estimated time for a shear wave to travel from the initiating crack to the pins and subsequently overtake the propagating crack, serves to identify t_A as the time of the arrival of the shear wave. This is illustrated in Fig. 7 where a sudden change in velocity is obtained at point A' corresponding to a jump in the stress intensity factor at point A. In some of the experiments performed, more than one jump in velocity and stress intensity factor was observed. In all specimens tested, the most intense of the jumps was always identified as the one corresponding to the arrival of the shear wave. The other crack tip velocity and stress intensity peaks were not positively identified.

The additional crack length Δl between the two steady states at the instant of arrival of the shear wave is due to loading device flexibility. A simple calculation was performed in which the compliance both of the specimen and of the loading mechanism were determined for the present specimen geometry and the present loading apparatus. By following the analysis of FREUND (1979), the jump was estimated to be of the order of 10 mm, a value found to hold consistently for all experiments.

To demonstrate the difference between experiments performed in steels and experiments performed in polymers, the calculation was repeated for a hypothetical polymer specimen. Both the specimen and loading device configurations were taken as identical to those in the experiments performed with the 4340 steel. For the polymer specimen, the ratio of the specimen flexibility to that of the loading device flexibility is very much lower than for a steel specimen. The calculation indicated that the effect of the reflected shear waves on the crack tip motion is indeed negligible, and that the loading device can be considered to be perfectly rigid. The prediction is consistent with experiments conducted in polymers and explains the lack of oscillations in the K_{Ic}^d and v values for these materials. The discussion demonstrates the advantages gained by keeping the ratio of specimen to loading device stiffness as low as possible.

At the onset of dynamic propagation, the crack accelerates very rapidly from zero velocity to the initial propagation velocity and the crack tip motion differs significantly from steady state. High accelerations at initiation cause the generation of Rayleigh surface waves at the crack tip. These waves propagate along the two faces of the crack

surface, i.e. down the cantilever arms, until they reach the corners of the specimen where they are partially reflected. FREUND (1981) as well as SCHMUELY *et al.* (1978) showed that these reflected waves can overtake the running crack and it has been suggested by various authors that they play an important role in the arrest process. The present experiments suggest that crack deceleration or arrest was coupled with the estimated arrival time, t_B, of the reflected Rayleigh wave. The experimental evidence is consistent with the predictions of the analysis, and provides some evidence that the Rayleigh waves may play a determining role in the crack arrest process.

7. CONCLUSIONS

A series of experiments has been described in which a crack was made to propagate rapidly in a set of DCB specimens of an AISI 4340 steel. The purpose of these tests was to obtain a direct measure of the stress intensity factor K_{Ic}^d during rapid crack propagation. This was effected by employing the shadow spot or caustics method which was adapted to the opaque specimens by viewing a reflected image. A high speed camera recorded a series of twelve photographs of the caustic patterns as the crack advanced and eventually arrested.

The results show that the dynamic stress intensity factor K_{Ic}^d is a monotonically increasing function of crack velocity. At low speeds the dependence of K_{Ic}^d on speed is small, but at the higher crack speeds it becomes quite pronounced. It is believed that this functional dependence of K_{Ic}^d on velocity is a material property. Evidence for this is presented. For instance, it is observed that the variations in the measured value of K_{Ic}^d during crack propagation correspond with variations in the observed crack velocity.

ACKNOWLEDGEMENT

The research support of the Office of Naval Research, through Grant N00014-78-G-0051 with Brown University, is gratefully acknowledged.

REFERENCES

BEINERT, J. and KALTHOFF, J. F. 1979 *Mechanics of Fracture* (edited by G. SIH), Noordhoff, Leyden.

COTTERELL, B. and RICE, J. R. 1980 *Int. J. Frac.* **16,** 155.

DAHLBERG, L., NILSSON, F. and BRICKSTAD, B. 1980 *Crack Arrest Methodology and Applications* (edited by G. T. HAHN and M. F. KANNINEN), ASTM, Philadelphia, 89.

DALLY, J. W. 1980 *Optical Methods in Mechanics of Solids* (edited by A. LAGARDE), Sijthoff & Nordhoff, 692.

DOUGLAS, A. S. 1982 PhD Thesis, Brown University.

FREUND, L. B. 1979 *Mathematical Problems in Fracture Mechnics* (edited by R. BURRIDGE), Am. Math. Soc. 21.

FREUND, L. B. 1979 *J. Mech. Phys. Solids* **25,** 69.

FREUND, L. B. 1981 *Int. J. Frac. Mech.* **17,** R83.

FREUND, L. B. AND DOUGLAS, A. S. 1982 *J. Mech. Phys. Solids* **30,** 59.

GLENNIE, E. B. 1972 *J. Mech. Phys. Solids* **20,** 415.
GOLDSMITH, W. and KATSAMANIS, F. 1979 *Exp. Mech.* **19,** 235.
KALTHOFF, J. F., BEINERT, J. and WINKLER, S. 1980 *Optical Methods in Mechnics of Solids* (edited by A. LAGARDE), Sijthoff & Nordhoff, 497.
KANNINEN, M. F. 1978 *Numerical Methods in Fracture Mechanics* (edited by A. R. LUXMORE and D. R. J. OWEN), Pineridge Press, Swansea, 612.
KOBAYASHI, A. S. 1970 *Exp. Mech.* **10,** 106.
KOBAYASHI, A. S. 1978 *Fracture Mechanics* (edited by N. PERRONE *et al.*), Univ. of Virginia Press, Charlottesville, 481.
KOBAYASHI, T. and DALLY, J. W. 1978 *Crack Arrest Methodology and Applications* (edited by G. T. HAHN and M. F. KANNINEN), ASTM, Philadelphia, 189.
MA, C. C. 1982 ScM Thesis, Brown University,
MANOGG, P. 1964 PhD Thesis, University of Freiburg (in German).
NISHIOKA, T. and ATLURI, S. N. 1982 *Engng Frac. Mech.* **16,** 303.
RAVI-CHANDAR, K. 1982 PhD Thesis, California Institute of Technology.
RAVI-CHANDAR, K. and KNAUSS, W. G. 1982 *Int. J. Frac.* **20,** 209.
RICE, J. R. and TRACEY, D. M. 1969 *J. Mech. Phys. Solids* **17,** 201.
ROSAKIS, A. J. 1982 PhD Thesis, Brown Univeristy.
ROSAKIS, A. J. and FREUND, L. B. 1981 *J. Appl. Mech.* **48,** 302.
ROSAKIS, A. J. and FREUND, L. B. 1982 *J. Engng Matls Tech.* **104,** 115.
SCHMUELY, P., PERETZ, D. and PERL, M. 1978 *Int. J. Frac. Mech.* **14,** R69.
THEOCARIS, P. S. and GDOUTOS, E. E. 1972 *J. Appl. Mech.* **39,** 91.